

## **The reactivity of mesoporous silica modified with acidic sites in the production of biodiesel**

Linda Sherry and James A Sullivan\*

UCD School of Chemistry and Chemical Biology, SFI SRC in Solar Energy Conversion,  
Belfield, Dublin 4, Ireland

\*[james.sullivan@ucd.ie](mailto:james.sullivan@ucd.ie), Tel: +353 1 716 2135, Fax: +353 1 716 2127

### **Abstract**

This work has studied a range of acidic catalysts which have been prepared through the modification of mesoporous silica materials. Specifically we have prepared  $\text{--SO}_3\text{H}$  modified materials (in the presence and absence of a hydrophobic component) and  $\text{--COOH}$  and  $\text{--CN}$  materials. We have characterized these catalysts using TEM, TGA, TPD of probe molecules and IR and we have analysed their activity in the esterification of octanoic acid and the transesterification of triacetin. Activity in the esterification reaction (in which all catalysts are active) is not determined by the acid site concentration of the catalyst while the activity of active catalysts in the transesterification reaction (in which only  $\text{--SO}_3\text{H}$  materials are active) appears related to acid site concentration.

**Keywords:** esterification, transesterification, modified mesoporous  $\text{SiO}_2$ , acid catalysts

## 1. Introduction

Combustion of fossil fuels is the source of ~90% of all our energy generation, with the transportation sector accounting for 29% of the overall figure [1]. Localised problems associated with the combustion of fossil fuels include the generation of air pollutants, with the greatest source of emissions coming from motor vehicles. Anthropogenic air pollutants include sulphur oxides, nitrogen oxides, carbon monoxide, volatile organic compounds and particulate matter – all of which result from the combustion of fossil fuels in the transport sector. The negative effects on human health due to poor air quality have been well documented with The World Health Organization stating that 2.4 million people die each year from causes directly attributable to air pollution, highlighting the seriousness of this problem [2].

Global issues arising from the combustion of fossil fuels are another serious problem. With the approach of peak oil production, we are undeniably facing the depletion of a valuable finite resource that currently also feeds the vital chemical, pharmaceutical, polymer, petrochemical and fertilizer industries. In 2007, transportation was the largest consumer of petroleum, with 14.3 million barrels per day of petroleum products being consumed for transportation purposes [1]. This highlights the fact that the excessive use of petroleum products in this manner is an extremely wasteful use of a dwindling resource. A second global issue relates to the emission of carbon dioxide which is a greenhouse gas. Carbon dioxide is the most important anthropogenic greenhouse gas with its annual emissions growing by ~80% between 1970 and 2004 [3]. This global increase in CO<sub>2</sub> concentration is mainly attributed to the combustion of fossil fuels. This has attracted much attention over the past 50 years due to the possible negative impacts associated with it, *i.e.* possible global warming, and many efforts are continuously being made to reduce the concentrations of

these greenhouse gas emissions, with the most commonly quoted being the Kyoto Protocol [4].

Biomass refers to living or recently dead biological matter which can be used as biofuel [5]. Biodiesel is the most common biofuel in Europe and is available in both its neat form (referred to as B100) or in blends with petroleum diesel [6]. The advantages of this fuel mitigate the majority of the problems associated with the combustion of fossil fuels, with the two most obvious effects being the reductions in the demand for non-renewable resources and the reduced emissions of CO<sub>2</sub> (considering it as a “carbon neutral” fuel). As well as mitigating these problems, biodiesel also has advantages associated with the diesel engine itself including reduced engine wear, improved lubricating qualities and more complete fuel combustion [7, 8]. Also, no modifications are required to the modern diesel engine for the replacement of petroleum derived diesel with biodiesel. Biodiesel is synthesized from the transesterification of triglycerides (found in oils and fats) with methanol in the presence of a catalyst. However, in order to make biodiesel more economically viable, there is a need for biodiesel feedstock to originate from biomass waste products, crops grown on currently non-arable land, animal fats (*i.e.* beef tallow) or even used vegetable oil [9].

Currently aqueous NaOH solutions are used as catalysts to promote transesterification and there are several problems associated with this catalyst. These include product separation from catalyst, the generation of large volumes of alkaline waste water and the formation of soap in the presence of free fatty acids in the feedstock [10 - 12]. Heterogeneous catalysis is an attractive solution to these problems [13-17]. Cheaper feedstocks which include waste vegetable oils and animal fats contain high concentrations of free fatty acids (which will lead to considerable soap formation in the presence of the NaOH<sub>(aq)</sub> catalyst). An ideal heterogeneous catalyst should be effective in the transesterification of triglycerides and also the esterification of fatty acids. Solid acidic catalysts are known to effectively promote the

esterification of free fatty acids [18-20] and it has been shown that solid basic catalysts are much more active in the transesterification reaction [21-23]. In this work we describe the preparation, characterization and application of a number of acidic mesoporous silicas which show activity in both reactions with the hope of producing a catalyst which can simultaneously (where required) transesterify and esterify cheaper feedstocks – containing both triglycerides and high concentrations of free fatty acids.

Mesoporous silicate structures were discovered by Mobil Research in 1992 [24] and much interest has been shown in these materials due to their high surface areas and uniformly sized pores which range in size between 2 – 50 nm. Catalytic properties, pore size, hydrothermal stability and flexibility in tuning the mesoscale and large-scale morphologies can all be modified through manipulation of surfactant and inorganic material concentrations, ionic strength, pH and the inclusion of non-polar species and other additives in the preparation mixture [25]. Unlike zeolite-type materials, whose pore sizes are constrained to the microporous range, these mesoporous silicates have the ability to allow larger reactants access to the internal surfaces where a high concentration of active sites can be incorporated, thereby providing catalytic activity. MCM-41 and SBA-15 are two of the most widely studied structures in this class of materials [24 – 29]. In this work it has been decided to use SBA-15 as our support material due to its structural and thermodynamic advantages over MCM-41[30]. We have grafted sulfonic acid, cyano- and carboxylic acid functionalities onto this support material using an *in-situ* synthesis method which has previously been described [26 - 29]. Due to the fact that water is a side product of the esterification reaction, it was decided to test the use of an additional hydrophobic group when modifying these materials. Previous work has been done in this area by Shanks *et al.* using various hydrophobic trialkoxysilanes in conjunction with the sulfonic acid functionalities in the esterification of palmitic acid. It was found that the method by which the hydrophobic group was

incorporated into the material and the size of the group played vital roles in the esterification reaction [31]. In this work we have used ethyl groups to introduce such hydrophobicity into our materials and we have furthered this study by varying the concentration of these surface ethyl groups in an attempt to understand what, if any, effect this has on the activity of the sulfonic acid material in the promotion of the esterification and transesterification reactions.

## 2. Experimental

### 2.1 Preparation of Catalysts

SBA-15 materials were synthesized using triblock copolymer Pluronic P123 ((EO)<sub>20</sub>(PO)<sub>70</sub>(EO)<sub>20</sub>) as a template (where EO refers to ethylene oxide and PO refers to propylene oxide) and tetraorthethylsilicate (TEOS) as the silica source. Surface modifications were introduced to the porous structure using an *in-situ* technique by adding variously functionalized trialkoxysilanes during the condensation of the hexagonal structure. The template was removed from these modified materials by a 24 h ethanol reflux. Unmodified SBA-15 was also prepared as detailed elsewhere [32] – one sample was left as synthesized with its template remaining in the pores (labeled As Synthesized), a second sample underwent a 24 h ethanol reflux to remove the template (labeled 24 Hr Reflux) and a final sample was subjected to a calcination procedure at 600 °C in air for 6 h (labeled Calcined). The two series of modified catalysts were synthesized as detailed below.

#### 2.1.1 SBA-15/SO<sub>3</sub>H/C<sub>2</sub>H<sub>5</sub>

4 g of P123 (0.00069 mols) was dissolved in 120 g of 1.9 M HCl and 30 g of H<sub>2</sub>O. Upon dissolution, 6.8 g of TEOS (0.0326 mols) was added and stirred for 45 minutes at 40 °C. 1.6 g of 3-Mercaptopropyltrimethoxysilane (MPTMS) (0.0081 mols), 2.5 g of H<sub>2</sub>O<sub>2</sub> (0.0735

mols) and varying amounts of ethyltrimethoxysilane (EtTMS) were then added such that the final molar composition became TEOS:0.8 MPTMS:0.2 P123:0.017 HCl:5.9 H<sub>2</sub>O:193 H<sub>2</sub>O<sub>2</sub>:1.8 EtTMS:X, where X = 0, 0.1 or 0.2. The reaction was stirred for 20 h at 40 °C and then aged at 80 °C for a further 24 h. The solid product was then filtered and air dried and the template was removed by reflux in 150 mLs of ethanol for 24 h. Throughout this manuscript, these materials are labeled SBA-15/SO<sub>3</sub>H (where X = 0), SBA-15/SO<sub>3</sub>H/C<sub>2</sub>H<sub>5</sub> (9.1%) (where X = 0.1) and SBA-15/SO<sub>3</sub>H/C<sub>2</sub>H<sub>5</sub> (16.7%) (where X = 0.2). (Here the value in parentheses indicates the mol % of the hydrophobic ethyl group in the silica fraction). These materials, albeit produced using different preparation conditions and containing different loadings of functional groups, should be similar to those previously produced by Shanks *et al.* [31] and used in esterification reactions.

#### 2.1.2 SBA-15/CN and SBA-15/CO<sub>2</sub>H

4 g of P123 (0.00069 mols) was dissolved in 120 g of 1.9 M HCl and 30 g of H<sub>2</sub>O. Upon dissolution 1.74 g of 2-(cyanoethyl)triethoxysilane (CETES) (0.008 mols) was added and stirred for 1 h at 40 °C. 6.8 g of TEOS (0.0326 mols) was then added such that the final molar composition became TEOS:0.8 CETES:0.2 P123:0.017 HCl:5.9 H<sub>2</sub>O:193. The remaining element of synthesis and template removal was carried out as discussed above in 2.1.1. However, in order to oxidize the cyano modified material to a carboxyl modified material, it was subject to a 24 h H<sub>2</sub>SO<sub>4</sub> (150 mLs of 49 wt. % solution) reflux. This treatment also acted as the template removal method for this material. These materials are labeled SBA-15/CN and SBA-15/CO<sub>2</sub>H. The preparation of a closely related material has been described previously by Schüth *et al.* [33].

## 2.2 Characterization of Catalysts

For TEM analysis all samples were dispersed in ethanol and sonicated for 10 minutes. A bead of the solution was then dropped onto holey carbon films supported by a TEM copper grip. This was allowed to evaporate prior to analysis. TEM was performed using a FEI Tecnai G2 20 Twin microscope operated at 200 kV.

BET analysis of the surface area of the calcined and refluxed samples was carried out on a Quantachrome Nova 2000E Series instrument. Previous literature [31, 33] suggests that the surface modifications we carry out have relatively small effect on textural properties.

Thermogravimetric analysis was carried out using a Q 500 Thermogravimetric Analyser (TA Instruments) on the unmodified samples in order to compare ethanol reflux with calcination as template removal methods. Samples were held in a flow of air and ramped from room temperature to 750 °C at a ramp rate of 10 °C/min, while the weight loss endured by the samples was monitored.

For NH<sub>3</sub> TPD, samples (20 mg) were loaded into a fixed bed quartz flow reactor which was housed in a furnace. The solid was held in place using quartz wool. Samples were subjected to a flow of He (100 mL min<sup>-1</sup>) at 80 °C for 30 minutes to remove any physisorbed species from the surface. The temperature was then lowered to 50 °C and samples were dosed with 3000 ppm of NH<sub>3</sub> in a flow of He (70 mL min<sup>-1</sup>) until saturated (~1 h). The NH<sub>3</sub> signal at this point was recorded as a calibration factor before the NH<sub>3</sub> flow was removed from the stream and replaced with He while the catalyst cooled to 30 °C. The catalyst was held at this temperature until the NH<sub>3</sub> signal had returned to baseline – this ensures the removal of the physisorbed fraction. When the mass spectrometer NH<sub>3</sub> signal returned to background levels, the sample was heated from 30 to 700 °C at a rate of 10 °C min<sup>-1</sup> while an online Prolab Mass Spectrometer continuously monitored a fraction of the exhaust gas. From the NH<sub>3</sub> desorption

profiles (from which the H<sub>2</sub>O contribution has been removed) we can relate the temperature and magnitude of desorption from the surface to the strength and concentration of the surface accessible acid sites.

FTIR spectra of all samples were carried out on a Vertex 70 (Bruker) in order to characterize the surface functionalities.

## 2.3 Catalytic Testing

Before all reactions were carried out, catalysts were left in the oven at 80 °C overnight.

### 2.3.1 Esterification Reaction

In this work octanoic acid was used as a model free fatty acid (FFA). A 20 CH<sub>3</sub>OH : 1 FFA wt. ratio was used with a catalyst loading of 10 wt. % (of FFA). A 100 mL round bottom flask was charged with 250 mg of catalyst and 50 g of methanol and was heated to 60 °C. 2.5 g of octanoic acid was preheated to 60 °C and then added to the flask. A condenser was added to the top of the flask and the reaction was stirred for 24 h, with aliquots being removed for analysis at specific time intervals.

### 2.3.2 Transesterification Reaction

In this work triacetin was used as a model triglyceride. A 9 CH<sub>3</sub>OH : 1 oil mole ratio was used with a catalysts loading of 1 wt. % (of oil). A 50 mL round bottom flask was charged with 168 mg of catalyst and 22.18 g of methanol and was heated to 60 °C. 16.8 g of triacetin was preheated to 60 °C and then added to the flask. A condenser was added to the top of the flask and the reaction was stirred for 24 h, with aliquots being removed at specific time intervals.



We have also carried out blank experiments in the absence of catalysts under the same reaction conditions. In the transesterification reaction no conversion to product was observed while in the esterification reaction, conversion to FAME was at least an order of magnitude lower, with a reactant to product conversion of 6.2% after 24 h (the lowest conversion in the presence of catalyst was  $\sim 55\%$ ).

### 2.3.3 Reaction Monitoring

$^1\text{H}$  NMR was used as a quantitative method to monitor the reaction progress. Aliquots were removed from the batch reaction every hour for 6 hours and again at 24 hours and were quenched on ice. Acetone was then added to each as an internal standard. The proton response under the acetone peak (2.17 ppm) was integrated and compared to that under the formed methyl ester peak (3.67 ppm).

## 3. Results and Discussion

### 3.1 TEM Imagery

All materials were studied using TEM. The hexagonal ordering was present in all catalysts and modification did not greatly affect either pore size or structure with all materials showing a pore size of between 5 – 9 nm. Typical TEM images can be seen in Fig. 1a (SBA-15 “24 Hr Reflux”) and 1b (SBA-15/ $\text{SO}_3\text{H}$ ).

### 3.2 Thermogravimetric Analysis

Thermogravimetric analysis gives a measure of the weight loss of a material when subject to a heat treatment under different atmospheres. This analysis was carried out on unmodified SBA-15 samples, *i.e.* those without any functionalisation, whose template had (a) not been removed, (b) been removed by the reflux method detailed in section 2.1 and (c) been removed by the calcination method discussed in section 2.1. BET surface areas of the calcined material and the material following a 24 h reflux in ethanol are shown as an inset to the plot. These are of the orders of magnitude previously reported for these materials [32]. Differential thermogravimetric plots can be seen in Fig. 2 for the “As Synthesized” sample (with the template still remaining in the pores), the “24 Hour Reflux” sample and the “Calcined” sample. The “As Synthesized” sample shows a 50% weight loss upon the heat treatment which indicates that 50% of this material is actually made up of the template in the pores. In order for this material to act as an effective catalyst this template has to be removed in order to allow the reactant molecules access to the modified surface of the pores. The material which underwent a 24 hour ethanol reflux showed a 19% weight loss upon heat treatment. This tells us that the ethanol reflux only removes approximately 60% of the template from the pores of this material. Finally, as expected the material which had been calcined showed a negligible weight loss confirming that the calcination procedure effectively removes all the template from the pores. However, this calcination method cannot be used in conjunction with the *in-situ* synthesis method described in section 2.1.1 and 2.1.2 as the functionalized moieties (which are tethered to the material using organic linker molecules) would be removed from the material along with the template. These plots confirm that the reflux treatment has removed the most labile of the template but leaves behind the material that needs the highest temperature to oxidise.

### 3.3 NH<sub>3</sub> TPD

NH<sub>3</sub> TPDs for both series of catalysts can be seen in Fig 3a (materials modified with sulfonic acid and ethyl groups) and 3b (materials modified with cyano groups and carboxylic acid groups). From Fig 3a we can clearly see that the SBA-15/SO<sub>3</sub>H material contains the highest concentration of acid sites with 1044 μmol of NH<sub>3</sub> g<sup>-1</sup> desorbed from the saturated catalyst. The addition of different surface concentrations of the C<sub>2</sub>H<sub>5</sub> functional group to this material decreases the concentration of acid sites. Theoretically similar levels of sulfonic acid species should be present in all cases, *i.e.* similar quantities of MPTMS precursor were used in all cases. The [R-C<sub>2</sub>H<sub>5</sub>] does affect the acid site concentration on the material. Upon increasing the [R-C<sub>2</sub>H<sub>5</sub>] from 9.1% to 16.7%, an increase in the quantity of desorbed NH<sub>3</sub> is observed (from 429 μmol g<sup>-1</sup> to 813 μmol g<sup>-1</sup>). This is a marked increase but still, the material which is most effective in adsorbing the basic probe gas is that which is modified only with sulfonic acid groups making it the most acidic catalyst in terms of acid site concentration.

Fig. 3b details how the acidity of the cyano modified material is changed when these groups are oxidized (by a reflux in H<sub>2</sub>SO<sub>4</sub>) to carboxylic acid. The NH<sub>3</sub> desorption profile for SBA-15/CN shows a relatively low concentration of very strong acid sites, with a total NH<sub>3</sub> desorption of 520 μmol g<sup>-1</sup>. Upon oxidation of this material with H<sub>2</sub>SO<sub>4</sub>, the NH<sub>3</sub> desorption profile was completely altered. The acid site strength was weakened but the material now has two different types of acid site (both showing a weaker interaction with the probe gas than the cyano modified material). The overall acid site concentration is increased with the H<sub>2</sub>SO<sub>4</sub> reflux causing an increase in the NH<sub>3</sub> accessible site concentration from 520 μmol g<sup>-1</sup> to 739 μmol g<sup>-1</sup>.

### 3.4 IR Spectroscopy

IR spectroscopy was used to confirm the grafting of the functional groups onto the surface of these materials. The collected spectra for the materials modified with sulfonic acid groups can be seen in Fig. 4a and those for the cyano/carboxyl modified materials can be seen in Fig. 4b.

The first range of peaks to be noted are those between  $1000\text{ cm}^{-1}$  and  $1300\text{ cm}^{-1}$ , which represent the Si-O-Si stretches and these are present in each of the 5 materials [34]. A further characteristic stretch found in these materials is present at  $2900\text{ cm}^{-1} - 3800\text{ cm}^{-1}$  representing silanol O-H groups [34]. Another band present in all 5 materials is that from  $2800\text{ cm}^{-1} - 3000\text{ cm}^{-1}$ . This band relates to C-H stretches and is present in all materials firstly due to the presence of P123 remaining in the pores and secondly due to the propyl chain incorporated with the functionalization of the materials [35]. This band is absent in calcined SBA-15.

There is a marked increase in the intensity of this band ( $2800\text{ cm}^{-1} - 3000\text{ cm}^{-1}$ ) within the various different SBA-15/SO<sub>3</sub>H/C<sub>2</sub>H<sub>5</sub> catalysts (Fig.4a). It can clearly be seen that as [R-C<sub>2</sub>H<sub>5</sub>] increases so too does the intensity of the C-H stretch. Vibrations relating to the SO<sub>3</sub>H functionality are also seen in these spectra at  $650\text{ cm}^{-1}$  [36]. These are absent in all other materials.

Fig. 4b confirms the transformation of the R-CN modified material upon H<sub>2</sub>SO<sub>4</sub> reflux. The C-N stretch ( $2248\text{ cm}^{-1}$ ) is considerably attenuated following the acid reflux and is replaced by the R-COOH vibration ( $1650\text{ cm}^{-1}$ ) [37].

### 3.5 Reaction Profiles

#### 3.5.1 Esterification Reaction

The reaction profiles for the 5 catalysts in the esterification reaction between  $\text{CH}_3\text{OH}$  and octanoic acid can be seen in Fig. 5. All 5 materials show some activity in this reaction. Both SBA-15/CN and SBA-15/ $\text{CO}_2\text{H}$  show similar profiles with their initial reaction rates being more active than that of the sulfonic acid modified materials. However, conversion over these two catalysts plateaus at a maximum conversion of  $\sim 60\%$  after 6 hours. No further reactant conversion takes place for the following 18 h in the reaction mixture.

Characterisations are ongoing in an attempt to determine what the reason for this change in activity is related to. To date analysis of TGA, FTIR and recycling experiments with the used catalysts have been inconclusive in explaining this feature. The conversion of a fresh batch of starting material using a recycled catalyst after 24 h reaction is comparable to that of the fresh catalyst. This suggests that no permanent deactivation of the catalyst, which might explain the zero rates of conversion between 6 h and 24 h, took place.

Conversion over the SBA-15/ $\text{SO}_3\text{H}/\text{C}_2\text{H}_5$  catalysts continues for 24 h with almost quantitative conversion to FAME being obtained on completion of the reaction. The profiles from the 2 materials grafted with  $\text{C}_2\text{H}_5$  are similar to one another with the catalyst with the higher  $[\text{R}-\text{C}_2\text{H}_5]$  showing slightly higher conversion. The final conversion from the catalyst containing no  $\text{C}_2\text{H}_5$  fraction is identical to that with the 16.7%  $\text{R}-\text{C}_2\text{H}_5$  fraction. However, the overall conversion V. time profile is quite different. Initially ( $t < 4$  h) the catalyst with no  $\text{C}_2\text{H}_5$  groups tethered to the surface is significantly less active than the alkane containing materials. This is quite a significant finding and implies that the hydrophobic ethyl groups do have a positive effect on the initial activity of this catalyst. However, after 4 h there is a marked increase in the rate of reaction over the catalyst without these additional groups. Further work is ongoing in an attempt to understand this improvement. In conjunction with the TPD data these profiles suggest that although catalyst acidity is an important factor in promoting this reaction, it cannot be directly correlated with activity.

### 3.5.2 Transesterification Reaction

The conversion vs. time profiles for the 5 catalysts in the transesterification reaction with triacetin can be seen in Fig. 6. In general, conversions here are significantly lower than they were in the analogous esterification reactions (above). This is not an unexpected result since transesterification reactions are better promoted by basic catalysts (as discussed in section 1 [21-23]). Also, unlike the esterification reaction discussed above not all of the catalysts are active in promoting this reaction. Both SBA-15/CN and SBA-15/CO<sub>2</sub>H show no promotional activity after 24 hours.

Reaction profiles for the materials containing both SO<sub>3</sub>H and C<sub>2</sub>H<sub>5</sub> groups again appear to be quite similar to one another indicating (as was the case in the esterification reaction above) that the concentration of the C<sub>2</sub>H<sub>5</sub> fraction is not an important factor in promotion of this reaction. Both these catalysts continue to catalyse the reaction up to 24 h with a final conversion of ~18% being obtained in each case. The catalyst containing only tethered SO<sub>3</sub>H (SBA-15/SO<sub>3</sub>H) again shows the highest conversion of reactant to product in this reaction. This catalyst is active for the entire duration of the experiment and yields a final conversion of ~85%.

For this set of catalysts, and this reaction, it would appear that, the acid site concentration does in some way correlate to the activity of the reaction, with the most active catalyst showing the highest concentration of acid sites. However the –COOH and CN catalysts (which show significant NH<sub>3</sub> adsorption) are inert.

## 4. Conclusions

In this work we have synthesized and characterized a number of modified mesoporous silicas and analysed their activity in promoting the esterification of free fatty acids and the transesterification of triglycerides. Both of these reactions result in the formation of Fatty Acid Methyl Esters (FAME) – a diesel fuel substitute.

Infrared spectra confirmed the presence of the expected functional groups and TEM imagery confirmed the presence of the porous hexagonal structure in all our materials.

TGA confirms that our chosen template removal method only removes 60% of the template from the pores. This may have an important effect on the catalytic properties of the catalysts. The *in-situ* synthesis method used in this work means our only option for template removal is extraction through reflux.

We have shown that all 5 materials synthesized were active in promoting the esterification reaction with a model fatty acid but only the materials modified with sulfonic acid groups were active in the transesterification of a model triglyceride. Surface acidity is an important factor but acid site concentrations only appear to be one factor in influencing reactivity in the transesterification reaction. The addition of a hydrophobic C<sub>2</sub>H<sub>5</sub> fraction to this material was designed to keep the water (a side product of the esterification reaction) out of the pores of these materials but it appears that its simultaneous addition with MPTMS, while being of benefit in the initial stages of the esterification reaction, is detrimental to activity in the transesterification reaction.

## Acknowledgements

The author would like to thank UCD SCCB for a research demonstratorship.

## References

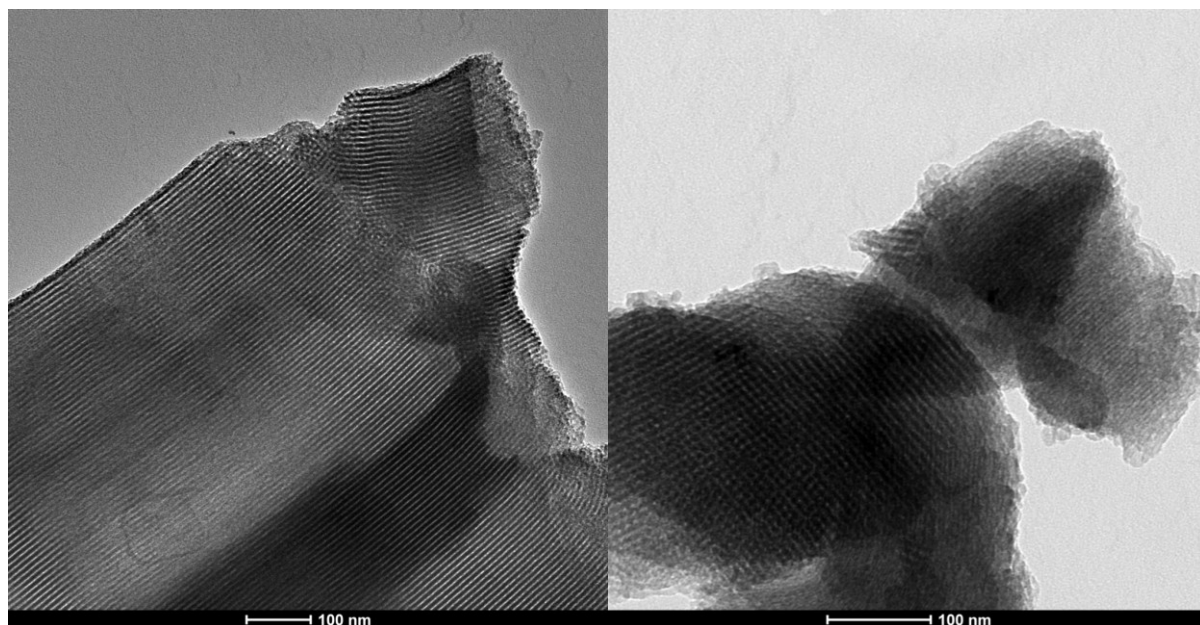
[1] Annual Energy Review 2007, Official Energy Statistics from the U.S. Government

- [2] [Estimated deaths & DALYs attributable to selected environmental risk factors, by WHO Member State, 2002](#)
- [3] Climate Change 2007, Synthesis Report, An Assessment of the Intergovernmental Panel on Climate Change
- [4] [Kyoto Protocol: Status of Ratification](#). [United Nations Framework Convention on Climate Change](#)
- [5] D.M. Alonso, J.Q. Bond and J.A. Dumesic, Green Chemistry, 12 (2010) 1493.
- [6] G. Fontaras, M. Kousoulidou, G. Karavalakis, T. Tzamkiozis, P. Pistikopoulos, L. Ntziachristos, E. Bakeas, S. Stournas and Z. Samaras, Environmental Pollution, 158 1451.
- [7] Leon Schumacher, Biodiesel Lubricity, University of Idaho
- [8] A.J. Kinney and T.E. Clemente, Fuel Processing Technology, 86 (2005) 1137.
- [9] M. Gürü, B.D. Artukoglu, A. Keskin and A. Koca, Energy Conversion and Management, 50 (2009) 498.
- [10] F.R. Ma and M.A. Hanna, Bioresource Technology, 70 (1999) 1.
- [11] M.J. Haas, A.J. McAloon, W.C. Yee and T.A. Foglia, Bioresource Technology, 97 (2006) 671.
- [12] M. D. Serio, M. Cozzolino, M. Giordano, R. Tesser, P. Patrono, E. Santacesaria, Industrial and Engineering Chemistry Research, 46, 2007, 6379
- [13] A.C. Carmo, L.K.C. de Souza, C.E.F. da Costa, E. Longo, J.R. Zamian and G.N. da Rocha, Fuel, 88 (2009) 461.
- [14] H.J. Kim, B.S. Kang, M.J. Kim, Y.M. Park, D.K. Kim, J.S. Lee and K.Y. Lee, Catalysis Today, 93-95 (2004) 315.
- [15] J.A. Melero, J. Iglesias and G. Morales, Green Chemistry, 11 (2009) 1285.
- [16] Y.M. Park, D.W. Lee, D.K. Kim, J.S. Lee and K.Y. Lee, Catalysis Today, 131 (2008) 238.
- [17] J.F. Puna, J.F. Gomes, M.J.N. Correia, A.P. Soares Dias and J.C. Bordado, Fuel, 89 3602.
- [18] J.M. Marchetti, V.U. Miguel and A.F. Errazu, Fuel, 86 906.
- [19] J.-Y. Park, D.-K. Kim and J.-S. Lee, Bioresource Technology, 101 S62.
- [20] Y.-M. Park, D.-W. Lee, D.-K. Kim, J.-S. Lee and K.-Y. Lee, Catalysis Today, 131 (2008) 238.
- [21] H.-J. Kim, B.-S. Kang, M.-J. Kim, Y.M. Park, D.-K. Kim, J.-S. Lee and K.-Y. Lee, Catalysis Today, 93-95 (2004) 315.
- [22] X. Liu, H. He, Y. Wang, S. Zhu and X. Piao, Fuel, 87 (2008) 216.



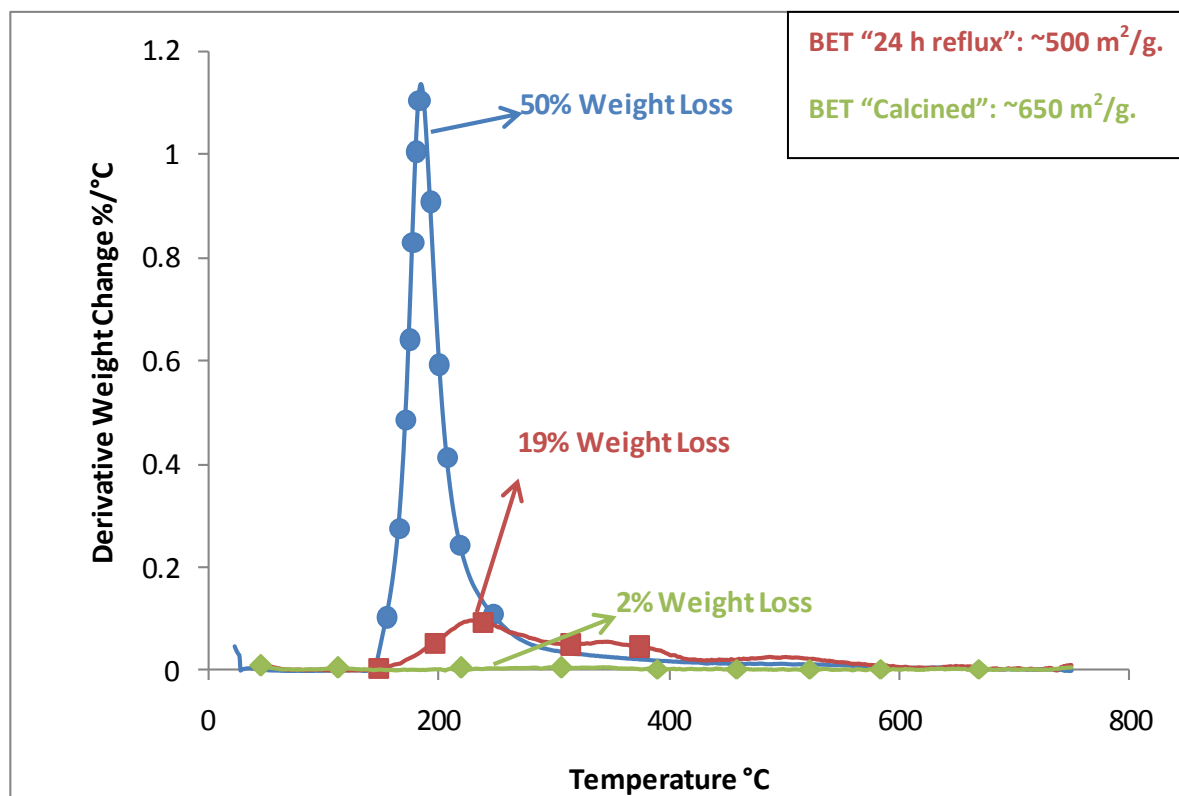
- [23] K. Noiroj, P. Intarapong, A. Luengnaruemitchai and S. Jai-In, *Renewable Energy*, 34 (2009) 1145.
- [24] C. T. Kresge, M. E. Leonowicz, W. J. Roth, J. C. Vartulia, J. S. Beck, *Nature*, 359, (1992), 710
- [25] K. J. Edler, *Australian Journal of Chemistry*, 58, (2005), 627
- [26] R.P. Hodgkins, A.E. Garcia-Bennett and P.A. Wright, *Microporous and Mesoporous Materials*, 79 (2005) 241.
- [27] A.S. Maria Chong, X.S. Zhao, A.T. Kustedjo and S.Z. Qiao, *Microporous and Mesoporous Materials*, 72 (2004) 33.
- [28] B. Rác, Á. Molnár, P. Forgo, M. Mohai and I. Bertóti, *Journal of Molecular Catalysis A: Chemical*, 244 (2006) 46.
- [29] C. M. Yang, B. Zibrowius and F. Schuth, *Chemical Communications*, (2003) 1772.
- [30] A. Galarneau, H. Cambon, T. Martin, L.-C.D. Ménorval, D. Brunel, F.D. Renzo, F. Fajula, A. Sayari and M. Jaroniec, *Studies in Surface Science and Catalysis*, Vol. Volume 141, Elsevier, 2002, p. 395.
- [31] I.K. Mbaraka and B.H. Shanks, *Journal of Catalysis*, 229 (2005) 365.
- [32] D. Zhao, J. Feng, Q. Huo, N. Melosh, G.H. Fredrickson, B.F. Chmelka and G.D. Stucky, *Science*, 279 (1998) 548.
- [33] C. Yang, Y. Wang, B. Zibrowius, F. Schüth, *Physical Chemistry Chemical Physics*, 6, (2004), 2461
- [34] Z. Wang, D. Wang, Z. Zhao, Y. Chen and J. Lan, *Computational and Theoretical Chemistry*, 963 403.
- [35] L.M. Yang, Y.J. Wang, G.S. Luo and Y.Y. Dai, *Microporous and Mesoporous Materials*, 84 (2005) 275.
- [36] L. Saikia, D. Srinivas and P. Ratnasamy, *Applied Catalysis A: General*, 309 (2006) 144.
- [37] Y.-C. Pan, H.-Y. Wu, L.-P. Lee, G.-L. Jheng, G.T.K. Fey and H.-M. Kao, *Microporous and Mesoporous Materials*, 123 (2009) 78.

Figure 1



**Figure 1a and 1b.** TEM images of SBA-15 “24 h Reflux” (1a) and SBA-15/SO<sub>3</sub>H (1b).

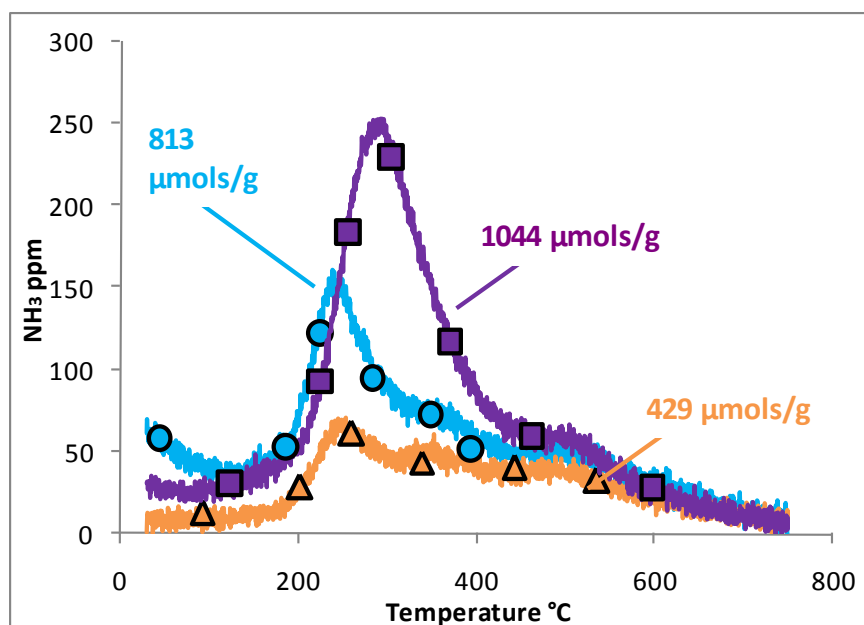
Figure 2



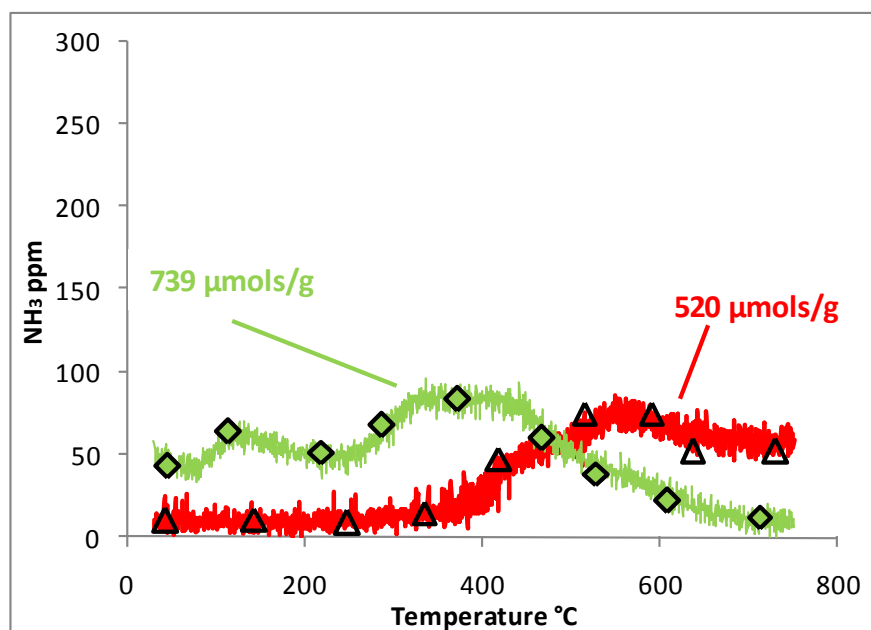
**Figure 2.** Differential Thermogravimetric plots of SBA-15 in air, As Synthesized (blue plot ●), 24 h Reflux (red plot ■) and Calcined (green plot ◆).

Figure 3

(a)



(b)




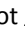
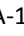
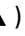
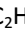
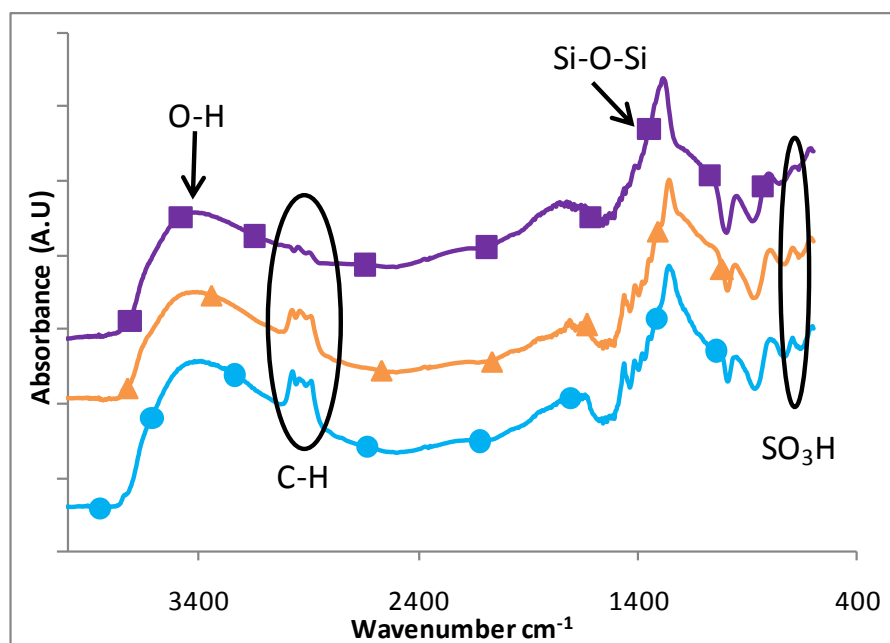
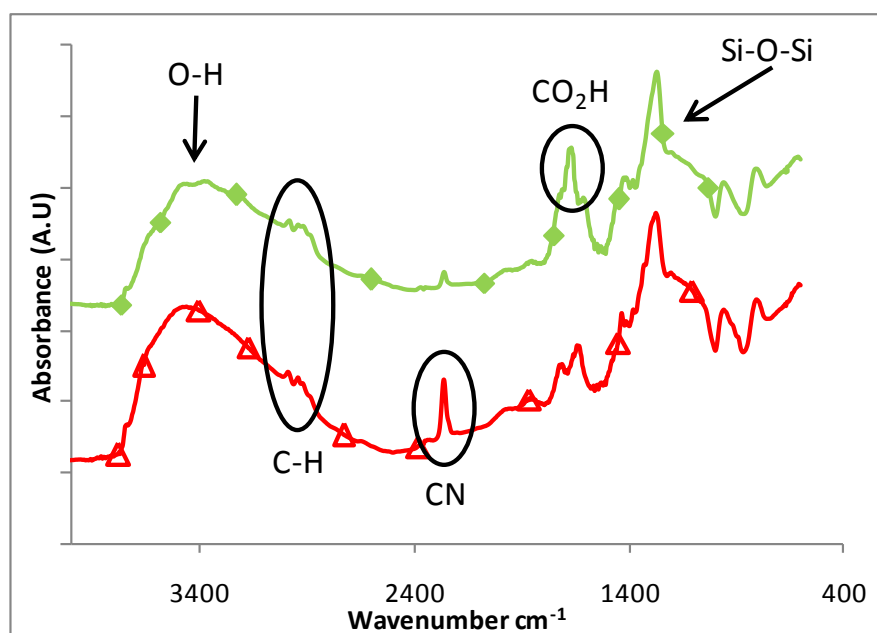
**Figure 3a** (a) NH<sub>3</sub> TPD profiles from SBA-15/SO<sub>3</sub>H (purple plot  ), SBA-15/SO<sub>3</sub>H/C<sub>2</sub>H<sub>5</sub> (9.1 %) (orange plot  ) and SBA-15/SO<sub>3</sub>H/C<sub>2</sub>H<sub>5</sub> (16.7 %) (blue plot  ) and (b) NH<sub>3</sub> TPD profiles for SBA-15/CN (red plot  ) and SBA-15/CO<sub>2</sub>H (green plot  )

Figure 4

(a)

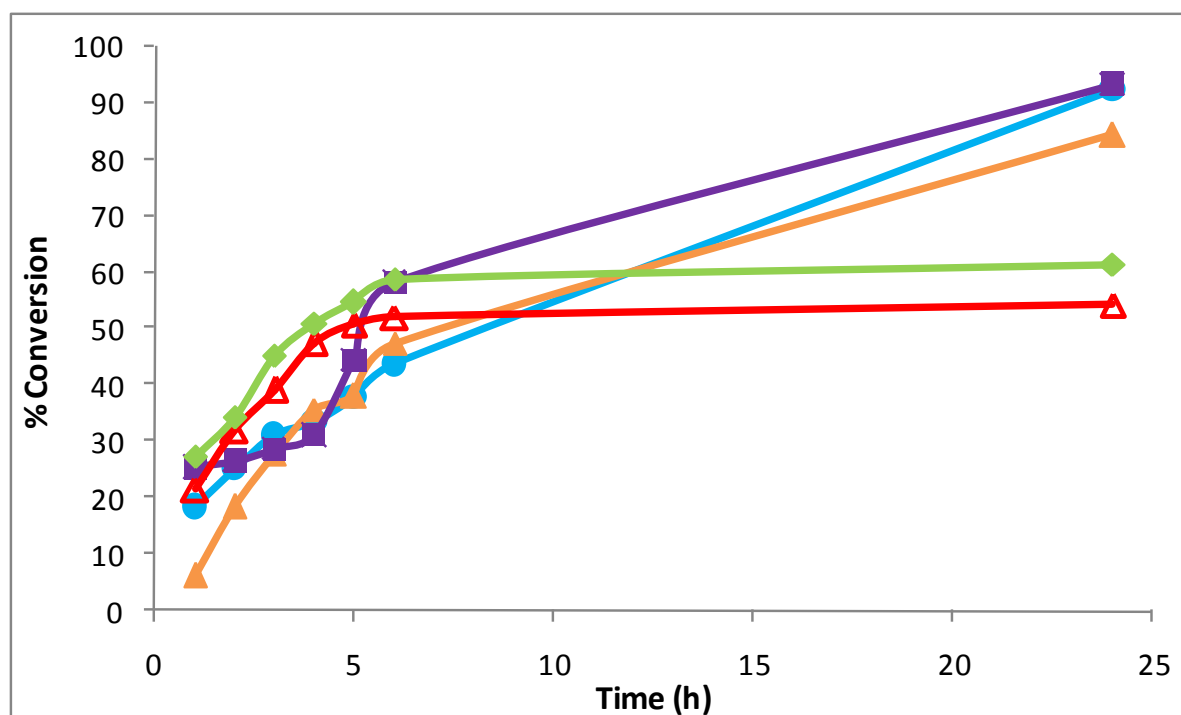


(b)



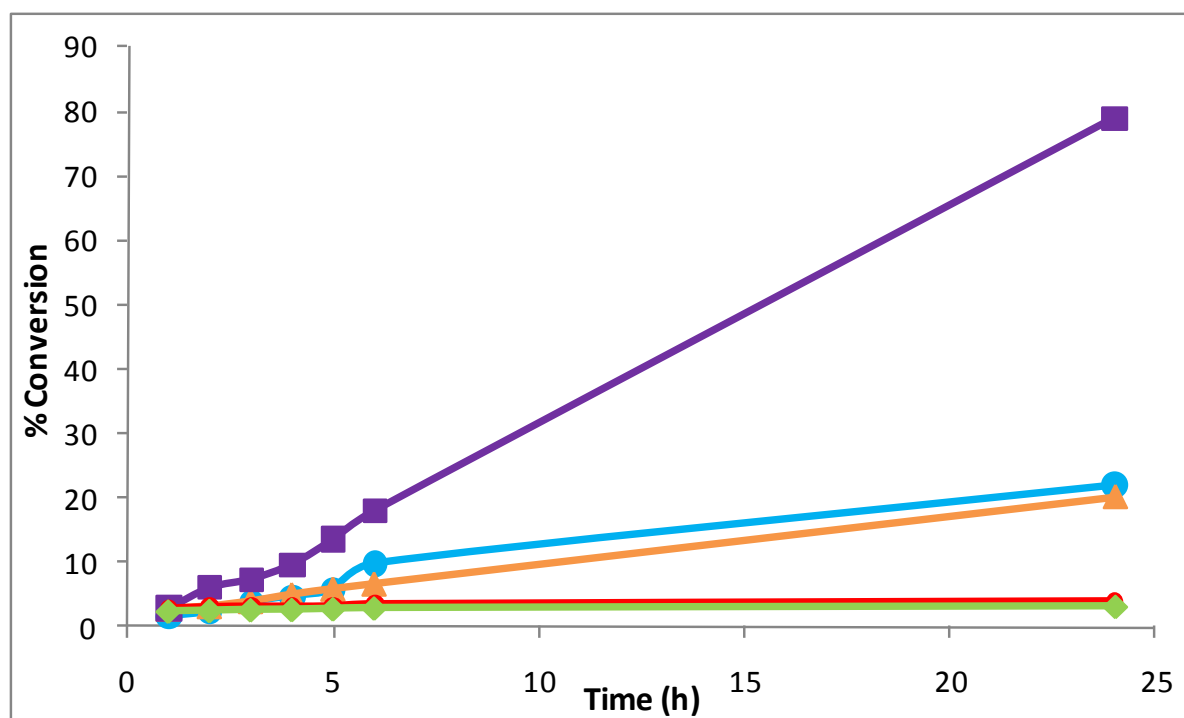
**Figure 4** (a) IR spectra of SBA-15/SO<sub>3</sub>H (purple plot ■), SBA-15/SO<sub>3</sub>H/C<sub>2</sub>H<sub>5</sub> (9.1 %) (orange plot ▲) and SBA-15/SO<sub>3</sub>H/C<sub>2</sub>H<sub>5</sub> (16.7 %) (blue plot ●) (b) IR spectra of SBA-15/CN (red plot ▲) and SBA-15/CO<sub>2</sub>H (green plot ◆)

Figure 5



**Figure 5.** Esterification reaction profiles for SBA-15/SO<sub>3</sub>H (purple plot ■), SBA-15/SO<sub>3</sub>H/C<sub>2</sub>H<sub>5</sub> (9.1 %) (orange plot ▲), SBA-15/SO<sub>3</sub>H/C<sub>2</sub>H<sub>5</sub> (16.7 %) (blue plot ●), SBA-15/CN (red plot ▲) and SBA-15/CO<sub>2</sub>H (green plot ◆)

Figure 6



**Figure 6.** Transesterification Reaction profiles for SBA-15/SO<sub>3</sub>H (purple plot ■ ), SBA-15/SO<sub>3</sub>H/C<sub>2</sub>H<sub>5</sub> (9.1 %) (orange plot ▲ ), SBA-15/SO<sub>3</sub>H/C<sub>2</sub>H<sub>5</sub> (16.7%) (blue plot ● ), SBA-15/CN (red plot ▲ ) and SBA-15/CO<sub>2</sub>H (green plot ◆ )